EPJ Web of Conferences **340**, 09022 (2025) https://doi.org/10.1051/epjconf/202534009022
Powders & Grains 2025

Particle-based modeling of continuum quasi-fragile matter fragmenting into granular-like packing

Gaël Combe[1,*], *Vincent* Richefeu[1,**], *Marta* Stasiak[1,***], *Gilles* Armand[2,****], and *Jad* Zghondi[2,†]

[1]Univ. Grenoble Alpes, CNRS, Grenoble INP, 3SR, 38000 Grenoble, France
[2]Andra, R&D Division, Meuse/Haute-Marne Underground Research Laboratory, 55290 Bure, France

Abstract. This work presents a numerical development of a two-dimensional particle-based model for simulating the mechanical failure of quasi-fragile materials. Inspired by Andra's industrial applications, the study focuses on perforated concrete blocks designed to enhance compressibility and stress dissipation. The numerical approach builds upon the Discrete Element Method (DEM), incorporating an interaction zone concept inspired by peridynamics to capture long-range forces beyond standard particle bonding techniques. The model effectively simulates the progressive failure process, from initial elastic loading to fragmentation, where evolving micro-cracks develop into macro-cracks, leading to the formation of freely moving fragments. A sensitivity analysis explores key parameters, including interaction zone size, energy dissipation, and microstructural variability. Applied to experimental concrete structures, this numerical investigation aids in optimizing perforation designs for industrial needs.

1 Introduction

This study contributes to the ongoing research efforts of Andra, the French agency for nuclear waste management. A key technological concept under investigation is the development of a compressible layer positioned between the bedrock and a concrete segment to optimize the structural integrity of deep tunnels. Andra explores various materials with high internal porosity, aiming to achieve mechanical stress reduction through extensive brittle damage.

Previous research has examined granular-based layers that allow for straightforward pre-casting into monolithic liners, but continuum-based alternatives remain a viable consideration. In this context, the present study focuses on the mechanical behavior of highly porous composite blocks, as illustrated in Figure 1(a).

To ensure the liner's longevity, the compressible layer undergoes extreme deformation, reaching up to 60% strain under mechanical compression. This process subjects the blocks to a prolonged quasi-brittle fracturing mechanism. The primary modeling challenge arises from the drastic transformation of the material, transitioning from a continuum to granular behavior.

At low strain levels, the block initially exhibits elastic deformation until micro-cracks begin to form and propagate. As strain increases, these micro-cracks evolve into an interconnected network of macro-cracks, eventually fragmenting the block into distinct units. These fragments move freely within the porous structure, leading to new long-range collisions. While continuum methods may be adequate at small strains, the need to capture large displacements and spontaneous contact interactions favors the Discrete Element Method (DEM) [1].

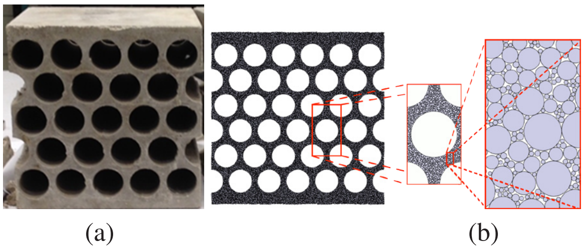

Figure 1. (a) Example of a compressible brick structure: a mortar block with a 15 cm side length featuring internal perforations of 20 mm diameter; (b) 2D model representation of the block with distributed circular perforations, see Table 1.

Although DEM is conventionally employed for modeling granular mechanics and particle breakage, it has also been successfully applied to simulate rocks and composite materials. To enhance its suitability for heterogeneous materials, long-range forces have been incorporated into the model through an interaction zone, a key concept inspired by Peridynamics [2].

2 Model

An in-house DEM algorithm solves Newton's second law of motion for individual rigid elements using the velocity-Verlet integration scheme. The problem is simplified

---

[*]e-mail: gael.combe@univ-grenoble-alpes.fr
[**]e-mail: vincent.richefeu@univ-grenoble-alpes.fr
[***]e-mail: ms-e@wp.pl
[****]e-mail: gilles.armand@andra.fr
[†]e-mail: jad.zghondi@andra.fr

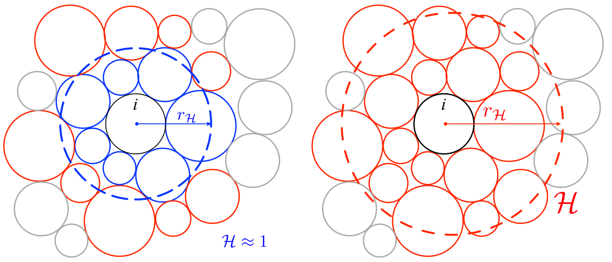

(a) (b)

Figure 2. Horizon is a finite, circular zone of influence of a given point i within which points can interact, marked by dashed line: (a) Short-range interactions are actually within an horizon of unit size. (b) Long-range neighbors will interact after widening the zone $\mathcal{H}$.

to a two-dimensional, gravity-free domain with periodic boundaries [3]. The discrete representation of the perforated bulk is constructed through a dense packing of rigid discs, as illustrated in Figure 1(b).

Figure 2 introduces the concept of the horizon $\mathcal{H}$, a finite circular interaction zone (dashed lines) characterized by the dimensionless parameter $r_{\mathcal{H}}/\langle d \rangle$, where $\langle d \rangle$ represents the mean disc diameter. In the conventional DEM framework, a small horizon value ensures that each disc i interacts only with its immediate physical neighbors, highlighted in blue in Figure 2(a). As the horizon increases, the central disc establishes interactions with a larger number of neighboring discs, as illustrated by the red discs in Figure 2(b). In classical DEM, contact forces are computed based on overlapping lengths, which becomes inadequate for long-range interactions. Consequently, extending the horizon necessitates a reformulation of the contact laws to properly account for long-range forces.

A key distinction between the method presented here and the DEM approach lies in the ability to break interaction bonds, even when they act over long distances, similar to peridynamics. In this hybrid model, when all interaction bonds connected to a given disc are broken, the disc ultimately behaves as an isolated rigid particle. This feature enables the opening and propagation of cracks, as in peridynamics. However, unlike peridynamics, this approach also allows for crack closure through re-contact, as fragments can interact again when they come into proximity. This re-contact mechanism enhances the model's ability to capture high compression rates by accounting for both fracture propagation and potential material reconnection under mechanical constraints.

Figure 3 summarizes the contact laws governing the constitutive behavior of cohesive interactions, referred to as bonds (with superscript $\bullet^{(b)}$). These bonds serve as either short-range or long-range interactions, ensuring material cohesion. Additionally, the bonds are capable of breaking, following a model inspired by Delenne's framework [4], which defines a linear elastic relationship between force and local displacements in both normal and tangential directions.

Geometry of the block structure	
Width L (m)	0.150
Height H (m)	0.150
Thinnest wall thickness $T_{\min}/\langle d \rangle$ (-)	10.514
Diameter of perforations (m)	0.02
Model parameters	
– Discretization –	
N_{disks} (-)	36 607
$d_{\max}$ (m)	0.001
$\langle d \rangle$ (m)	0.5044×10^{-3}
$d_{\max}/d_{\min}$ (-)	3
$\mathcal{H}$ (-)	3
Mean number of bonds per disc (-)	21.034
– Interactions –	
$k_n^{(b)} = k_n^{(c)}$ (N/m)	2.195×10^7
$k_t^{(b)} = k_t^{(c)}$ (N/m)	8.246×10^6
μ (-)	0.4
δ_n^0 (m)	1.529×10^{-6}
δ_t^0 (m)	7.7996×10^{-6}
α (-)	4
ζ_{max} (-)	1.1
– Perlin noise (when applied) –	
Length ℓ (m)	$9.989\langle d \rangle$
Smoothness Δ (-)	1.8
– Damping –	
Cundall damping coefficient (-)	0.7
Viscous damping rate (-)	0.9

Table 1. Geometrical and mechanical parameters of the model (see Figure 3 for additional explanations).

In contrast to the original framework, material failure is governed by a critical deformation state, as illustrated in Figure 3. In each direction, bond rupture is initiated at the critical stretch $\delta_\bullet^0$, marking the end of the elastic regime. Consequently, the critical force $f_\bullet^0$ results from an appropriate calibration of the material elasticity, $k_\bullet^{(b)}$. The current model introduces a rupture delay [5], wherein a dimensionless parameter ζ_{max} that regulates the shift of the yield surface. If ζ_{max} is set to unity, the bond vanishes instantaneously, and the failure envelope corresponds to the black curve in Figure 3. Increasing ζ_{max} allows the damage parameter D to evolve from 0 to 1. As a result, the rupture force is attenuated when the rupture envelope φ (depicted by the red curve) is reached.

3 Preliminary results

Preliminary tests were conducted to investigate the influence of different parameters on the mechanical response, whether considering macroscopic elasticity parameters or fracture patterns. However, due to space constraints, a detailed analysis of these aspects cannot be presented here. Instead, we will demonstrate the capabilities of the approach through a comparison of axial compression tests

https://doi.org/10.1051/epjconf/202534009022

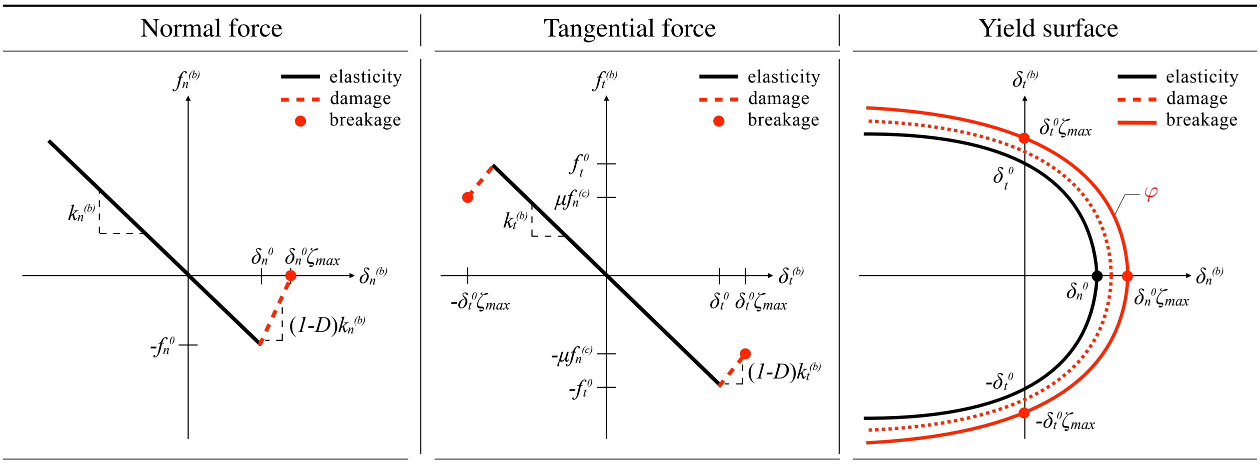

$$f_n^{(b)} = (1-D)\, k_n^{(b)}\, \delta_n^{(b)},$$
$$\text{where } \delta_n^{(b)} = l_n^0 - l_n$$

$$f_t^{(b)} = (1-D)\, k_t^{(b)}\, \delta_t^{(b)}$$

$$\varphi = \frac{\delta_n^{(b)}}{\delta_n^0\zeta_{max}} + \left(\frac{\delta_t^{(b)}}{\delta_t^0\zeta_{max}}\right)^{\alpha} - 1$$
breakage for $\varphi = 0$

Figure 3. Bond force laws – discrete forces and yield surface. Notation: superscript $\bullet^{(b)}$ stands for "bond", $\bullet^{(c)}$ stands for "contact", the power α tune the yield surface φ, δ_n^0 is the critical bond extension (pure tension), δ_t^0 is the critical bond shear displacement, $\delta_n^{(b)}$ and $\delta_t^{(b)}$ are normal and tangential bond variation (extension or shortening), ζ_{max} is the failure-delay factor, D is the damage parameter, $f_n^{(b)}$ and $f_t^{(b)}$ are tangential and normal bond forces and $k_n^{(b)}$ and $k_t^{(b)}$ are tangential and normal bond stiffnesses.

on bricks with slightly different perforation patterns. The differences lie in the symmetry, spatial distribution, and size of the perforations, without attempting to justify these choices, as they are part of an optimization study conducted for the needs of Andra.

From the material model calibration, three essential points emerge:

(*i*) The chosen level of bulk discretization is determined by the thinnest wall between the perforations, characterized by T_{min}; see Table 1.
(*ii*) The numerical sample must achieve a physically realistic ratio of tensile to compressive bearing capacities, σ_t/σ_c, which results from the interplay between $\delta_\bullet^0$ and ζ_{max}.
(*iii*) The horizon can be analyzed as a discretization parameter, exhibiting some correlation with all constitutive parameters.

The numerical simulation of oedometric compression are presented for the conditions and parameters summarized in Table 1.

Following our initial compression simulations on bricks with symmetrical structures, we observed that the resulting fracture patterns also displayed a degree of symmetry. Consequently, the macroscopic compression curve, shown in Figure 4, did not match our expectations (*i.e.*, it significantly differed from some experimental measurements we had). In particular, the compression stress dropped to zero. The elastic stress distribution within the block is distributed uniformly due to a constant, semi-symmetric spacing of the voids. Since, the rupture parameters were kept constant for all the bonds, the global failure occurred around all the perforation line at once. Then, the structure lacks stable frictional contact chain between the fragments and no load can be transfer through the samples.

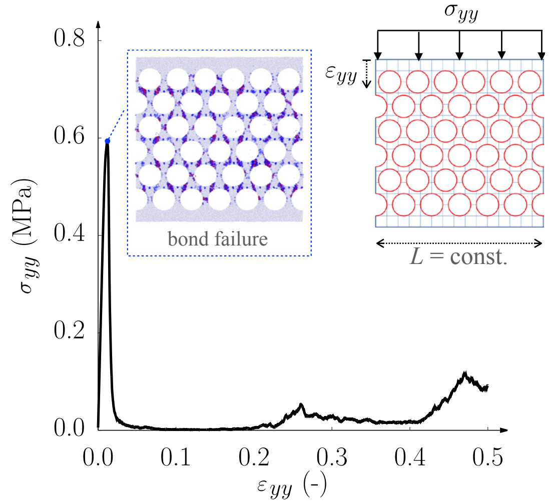

Figure 4. Macroscopic strain-stress compression curve for a brick with a symmetric perforation pattern. The horizon is $\mathcal{H} = 3$ and other parameters are in Table 1.

At this point the model lacks random imperfections cause by micro-cracks of composite materials.

To address this issue, we introduced a degree of heterogeneity in the material. However, this heterogeneity needed to maintain spatial coherence. To achieve this, we modulated the strength thresholds using Perlin noise. Perlin noise is a gradient noise function commonly used in computer graphics to generate natural-looking textures and patterns [6]. It provides smoothly varying random values, ensuring spatial consistency in the introduced heterogeneity. This characteristic makes it particularly suitable for controlling mechanical properties in numerical simulations.

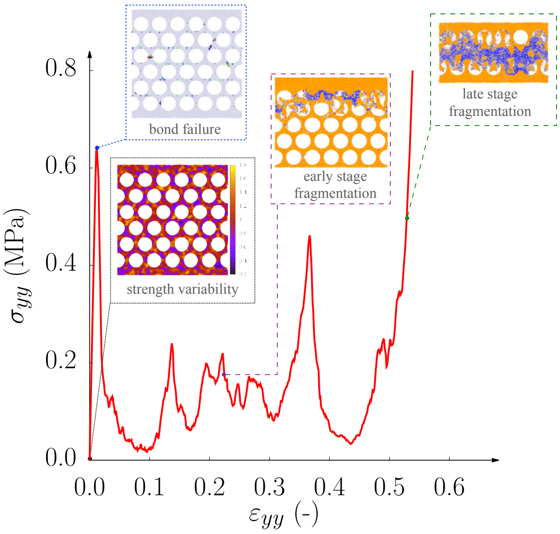

Figure 5. Macroscopic stress-strain compression curve for a brick with a symmetric perforation pattern, where the failure thresholds have been spatially distributed using Perlin noise (The horizon is $\mathcal{H} = 3$ and other parameters are in Table 1).

To highlight the benefits of incorporating heterogeneity into the material model, Figure 5 illustrates the resulting macroscopic compressive strength curves as a function of axial strain. The figure contrasts the case without heterogeneity in the failure thresholds. This comparison clearly reveals that the fracturing behavior, along with the material's overall response to compression, experiences a significant and advantageous change when heterogeneity is introduced. At the elastic regime's ending point, the fracture pattern was less intense as proven by the "bond failure" inset in Figure 5. Thus, the fragments were able to recontact and the mechanical curve exhibits the intermediate peaks, till the extensive breakage phase finishes for an advanced strain state; $\varepsilon_{yy} \approx 0.45$. Afterward, solely the increase of stress was captured.

It remains unclear, however, what the appropriate parameters should be for the Perlin noise. This is an intriguing question that would require a comprehensive investigation. The values given in Table 1 were selected as an arbitrary compromise resulting from a sensitivity analysis. Nevertheless, given our concerns regarding the simulation durations, which take about half a month with all precautions for stable simulations, it is not advised to use zone of interactions larger than $\mathcal{H} = 3$ (in 2D). This size already results in an average of 23 links per disc.

4 Concluding remarks

This study presents a novel numerical approach to simulate the mechanical failure of quasi-fragile materials, particularly focusing on perforated concrete blocks used in applications such as underground waste management. By combining the Discrete Element Method (DEM) with a long-range interaction zone inspired by Peridynamics, the model is able to capture the complex progressive failure mechanisms that characterize these materials, including crack propagation and fragmentation.

A sensitivity analysis performed in this study (not presented here due to space constraints) highlights the significance of several key parameters, including the interaction zone size, energy dissipation, and the effects of micro-structural heterogeneity. Furthermore, the introduction of spatially distributed failure thresholds, achieved using Perlin noise, has shown to significantly alter the material's response to compression. This modification provides valuable insights into the behavior of perforated concrete blocks under mechanical stress.

While the preliminary results indicate that the heterogeneity introduced by Perlin noise leads to more realistic fracture patterns and macroscopic behavior, further investigation is required to identify the optimal parameter values for the Perlin noise function.

Finally, the issue of simulation duration remains a challenge, with long simulation times necessitating trade-offs in model complexity. To support a computational affordability of this new approach, the maximum recommended size of the horizon is set to three mean diameters of the constituent discs.

Looking ahead, future work will focus on optimizing the balance between computational efficiency and model accuracy. More extensive studies are also needed to refine the implementation of heterogeneity and further explore its influence on material failure mechanisms. Ultimately, this model has the potential to aid in the design of more efficient and reliable perforated concrete structures, offering valuable insights for applications in the nuclear waste management sector and beyond.

References

[1] P.A. Cundall, O.D.L. Strack, A discrete numerical model for granular assemblies, Géotechnique **29**, 47 (1979).
[2] S. Silling, Reformulation of elasticity theory for discontinuities and long-range forces, J Mech Phys Solids **48**, 175 (2000).
[3] F. Radjaï, C. Voivret, in *Discrete-element modeling of granular materials*, edited by F. Radjaï, F. Dubois (Wiley-Iste, London, 2011), pp. 181–198
[4] J.Y. Delenne, Ph.D. thesis, Université Montpellier II - Sciences et Techniques du Languedoc (2002)
[5] C. Couture, Ph.D. thesis, Université Grenoble Alpes (2020)
[6] K. Perlin, An image synthesizer, ACM SIGGRAPH Computer Graphics **19**, 287 (1985).